Incessant acceleration of relativistic ions by an oblique shock wave

Shunsuke Usami, Hiroki Hasegawa, and Yukiharu Ohsawa[a)]
Department of Physics, Nagoya University, Nagoya 464-8602, Japan

(Received 12 December 2000; accepted 9 March 2001)

Motions of nonthermal, fast ions in an oblique shock wave are studied theoretically and numerically. After the encounter with a shock wave, some of the fast ions get to move with it. Their energies then increase once in each gyroperiod. Their momenta parallel to the magnetic field also increase. Thus, these particles eventually escape, going away ahead of the wave. However, it is theoretically predicted that under certain circumstances, owing to relativistic effects, particles cannot go faster in the direction of the shock propagation than the wave. Some particles therefore cannot escape from the wave. Accordingly, the acceleration could be repeated indefinitely. This idea is examined by means of a one-dimensional, relativistic, electromagnetic, particle simulation code with full ion and electron dynamics. The simulations demonstrate that the repeated acceleration of relativistic ions does occur. The acceleration processes were observed to continue until the end of simulation run. Also, it is shown that as the theory predicts, a higher energy particle can gain a greater amount of energy. © *2001 American Institute of Physics.* [DOI: 10.1063/1.1369120]

I. INTRODUCTION

Motivated by the observations of high-energy particles in astrophysical plasmas[1–5] or by the idea of plasma-based accelerators,[6,7] intensive theoretical and computational studies have been made by many authors.[8–25] Stochastic acceleration models such as Fermi acceleration have been often discussed for the production of cosmic rays.[8–11] Simulation studies, however, have revealed that there are various nonstochastic, particle acceleration mechanisms in large-amplitude plasma waves with coherent structure.[12–25]

In a multi-ion-species plasma like space plasmas, where hydrogen is the major ion component, a magnetosonic shock wave can accelerate some hydrogen ions via reflection by the large electric potential,[12–17,26–28] all the heavy ions by the transverse electric field,[18,19] and some electrons by longitudinal and transverse electric fields.[20,21] Since the magnetosonic wave is one of the most fundamental waves in astrophysical plasmas, these acceleration mechanisms are believed to play an important role in the production of high-energy particles in interplanetary, solar, and astrophysical plasmas.

Furthermore, it was found that a shock wave can further accelerate nonthermal, fast ions by a mechanism[22–25] different from the above three. In a shock wave propagating perpendicular to a magnetic field, fast ions barely entering the shock wave gain energies from the transverse electric field.[22] These fast ions can return to the upstream region from the shock wave because their speeds are much faster than the shock propagation speed v_{sh}. While they are in the shock region, they move in the direction nearly parallel to the transverse electric field formed in the wave; thereby they gain energy. (They eventually move to the downstream region after a while.) When particles encounter with a shock wave propagating obliquely to a magnetic field, some fast ions can get to move with it for some periods of time, several gyroperiods, and be accelerated several times by the transverse electric field;[23–25] these particles experience energy jump once in each gyroperiod while they are moving with the wave.[25] In this process, particle momentum parallel to the magnetic field, $p_{\|}$, increases at the moments when the particle goes in the shock wave and goes out to the upstream region.[23,24] Hence, after moving with the shock wave, the fast particle goes away ahead of it. It is because the particle velocity (averaged over a gyroperiod) in the direction of the wave normal is given by $\sim v_{\|}\cos\theta$, where $v_{\|}$ is the velocity parallel to the magnetic field and θ is the angle between the magnetic field and the wave normal.

However, the magnitude of parallel velocity $v_{\|}$ is limited by the speed of light c, even if $p_{\|}$ is increased indefinitely. Owing to this relativistic effect, under certain situations, the time-averaged fast-ion velocity in the direction of the wave normal cannot exceed the shock propagation speed v_{sh}, i.e., fast ions moving with the shock wave cannot escape from it. It is therefore expected that these particles could suffer repeated acceleration indefinitely, unless some other effects such as slowing down of the shock speed are given to this process. This paper investigates this phenomenon by theory and simulation.

In Sec. II, we describe physical processes leading to the acceleration of fast ions and give a theoretical estimate for the magnitude of an energy jump. Also, we derive conditions under which the indefinitely repeated acceleration can take place. In Sec. III, by using a one-dimensional (one space coordinate and three velocity components), relativistic, electromagnetic, particle simulation code with full ion and electron dynamics, we demonstrate that some fast (relativistic) ions can move with an oblique shock wave for very long periods of time and be accelerated many times. During the simulation run, the acceleration processes continued without cease. Also, we show that a higher energy particle can obtain

a)Electronic mail: ohsawa@phys.nagoya-u.ac.jp

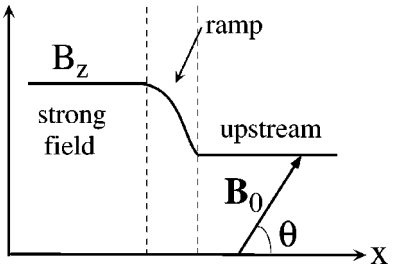

FIG. 1. Schematic shock profile. Width of the shock ramp is much smaller than gyroradius of a fast ion.

a greater amount of energy. In Sec. IV, we will summarize our work.

II. CONDITIONS FOR INCESSANT ACCELERATION

A. Physical considerations

For the definiteness, we assume that the external magnetic field is in the (x,z) plane,

$$\boldsymbol{B}_0 = B_0(\cos\theta, 0, \sin\theta), \tag{1}$$

with the angle θ in the region $0<\theta<\pi/2$ and that the shock wave is propagating in the x direction $(\partial/\partial y=\partial/\partial z=0)$ with a propagation speed $v_{\rm sh}$. We then consider the motion of a fast ion whose speed v is higher than $v_{\rm sh}$; and therefore much higher than the Alfvén speed $v_{\rm A}$,

$$v \gg v_{\rm A}. \tag{2}$$

A fast particle entering the shock region can return to the upstream region again, because of the gyromotion with $v \gg v_{\rm sh}$.

Relation (2) gives another important effect. Let ρ be the gyroradius and ω_{ci} be the relativistic ion gyro-frequency,

$$\omega_{ci} = q_i B/(m_i c\gamma), \tag{3}$$

with B the magnetic field strength and γ the Lorentz factor,

$$\gamma = (1 - v^2/c^2)^{-1/2}, \tag{4}$$

then substitution of the relation $v \sim \rho\omega_{ci}$ in Eq. (2) yields

$$\rho \gg c/\omega_{pi}, \tag{5}$$

where ω_{pi} is the ion plasma frequency. Because the width of the transition region (shock ramp) of an oblique shock wave is of the order of the ion skin depth c/ω_{pi}, Eq. (5) means that the gyroradius of a fast ion is much greater than the ramp width. The shock profile can thus be approximated by a step function when we analyze the motion of a fast ion. We will call the region immediately behind the thin shock ramp the strong field region, where the magnetic field, transverse electric field, electric potential, and plasma density have high values (see Fig. 1). The term ''shock region'' in this paper includes the shock ramp and strong field region. Roughly speaking, these quantities, B_z, E_y, φ, and n, have similar profiles in the laboratory frame, while B_y, E_x, and E_z are proportional to $\partial B_z/\partial x$.[20,29,30]

By virtue of these effects, it can be shown that the parallel momentum of a fast ion,

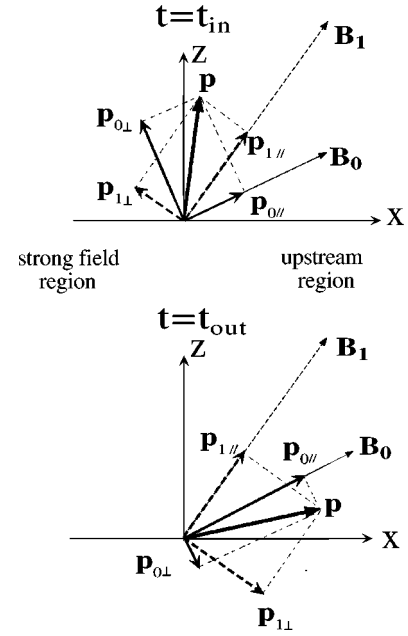

FIG. 2. Schematic diagram of magnetic fields and momenta at $t=t_{\rm in}$ and at $t=t_{\rm out}$. They are projected on the (x,z) plane. Because $B_{1z}>B_{0z}$, $p_\parallel$ increases.

$$p_\parallel = \boldsymbol{p}\cdot\boldsymbol{B}/B, \tag{6}$$

always increases when the particle enters and goes out of the shock region.[25,23,24] If the particle goes into the shock region at $t=t_{\rm in}$ and goes back to the upstream region at $t=t_{\rm out}$, then the increase in $p_\parallel$ in these processes is given by

$$\delta p_\parallel = [\boldsymbol{p}_{1\perp}(t_{\rm out}) - \boldsymbol{p}_{1\perp}(t_{\rm in})]\cdot\boldsymbol{B}_0/B_0, \tag{7}$$

where $\boldsymbol{p}_{1\perp}$ is the perpendicular momentum measured in the strong field region.[25] The subscripts 0 and 1 refer to quantities in the upstream and strong field regions, respectively. Because $\boldsymbol{p}(t)$ is continuous, we have $\boldsymbol{p}=\boldsymbol{p}_{0\parallel}+\boldsymbol{p}_{0\perp}=\boldsymbol{p}_{1\parallel}+\boldsymbol{p}_{1\perp}$ at $t=t_{\rm in}$ and at $t=t_{\rm out}$. Figure 2 shows a schematic diagram of $\boldsymbol{p}$ and $\boldsymbol{B}$ at $t=t_{\rm in}$ (upper picture) and at $t=t_{\rm out}$ (lower picture). We note that B_{1z} is greater than B_{0z} in a shock wave.[20,29,30] Evidently, $\boldsymbol{p}_{1\perp}(t_{\rm in})\cdot\boldsymbol{B}_0<0$ and $\boldsymbol{p}_{1\perp}(t_{\rm out})\cdot\boldsymbol{B}_0>0$. Hence, the left-hand side of Eq. (7) is positive; thus, $\delta p_\parallel>0$. Because of this effect, time-averaged velocity in the x direction, $\sim v_\parallel\cos\theta$, increases, and some of the fast ions begin to move with the shock wave after the encounter with it.

Another important process takes place while the particle is in the shock region, i.e., during the time from $t=t_{\rm in}$ to $t=t_{\rm out}$. The particle gains a large amount of energy from the transverse electric field; to which the gyration velocity there is roughly parallel.

Accordingly, if a fast ion encounters a shock wave, firstly, some fraction of $p_\perp$ of the particle is transferred to $p_\parallel$ at $t=t_{\rm in}$. Secondly, $p_\perp$ is increased in the strong field region. Thirdly, at $t=t_{\rm out}$, some fraction of $p_\perp$ is converted to $p_\parallel$ again, and the particle goes out to the upstream region. Owing to the gyromotion, it can enter the shock region again and undergo the same processes. Figure 3 illustrates orbit of a fast ion moving with and being accelerated by a shock

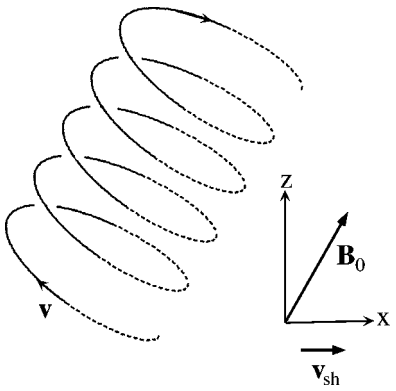

FIG. 3. Illustration of fast ion orbit moving with a shock wave. The orbit in the shock region is denoted by the solid line where the acceleration takes place, while the one in the upstream region is denoted by the dotted line. Strictly speaking, the gyromotions in the shock and upstream regions are not in the same plane.

wave. If the particle moves with the shock wave for a long period of time, these processes would be repeated many times; it would occur if the particle velocity has the relation

$$v_{\parallel}\cos\theta \sim v_{\mathrm{sh}}. \tag{8}$$

Particles with $v_{\parallel}\cos\theta < v_{\mathrm{sh}}$ will be caught up with by the shock wave if they are initially in the upstream region. Because $p_{\parallel}$ (and hence $v_{\parallel}$) is increased on the collision with the shock wave, relation (8) will be satisfied for some particles after the collision. They will get to move with the shock wave. When $v_{\parallel}$ becomes sufficiently large, $v_{\parallel}\cos\theta > v_{\mathrm{sh}}$, the particles go away ahead of the shock wave.

We show in Fig. 4 such an example obtained from a particle simulation; the method and detailed results of particle simulations will be described in the next section. The dotted line in the upper panel represents the location of the shock front propagating in the x direction with a propagation angle $\theta = 45°$. The solid line represents the x position of a fast particle; x is normalized to c/ω_{pe}. The oscillation of x is due to the gyromotion. The particle is in the upstream region initially and encounters the shock wave at $\omega_{pe}t = 480$. However, it quickly goes out to the upstream region at $\omega_{pe}t = 580$. It again enters the shock region at $\omega_{pe}t = 920$ and soon returns to the upstream region. It then goes away ahead of the shock wave. The bottom panel shows that the energy γ rapidly increases while the particle is in the shock region.

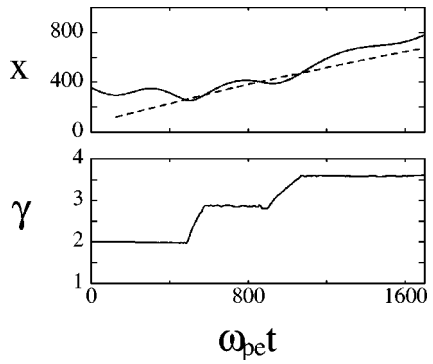

FIG. 4. Time variations of x position and Lorentz factor γ of a fast ion.

The particle speed, however, cannot exceed the speed of light c. Hence, if the propagation angle θ and shock speed v_{sh} have the relation

$$c\cos\theta \sim v_{\mathrm{sh}}, \tag{9}$$

then no particle would go away ahead of the shock wave. In this case, particles with $v_{\parallel} \sim c$ could move with the shock wave for extremely long periods of time, during which they would gyrate many times and be accelerated many times. The acceleration will occur once in each gyroperiod.

B. Magnitude of energy jump

We now estimate the amount of energy that a particle gains through the motion in the strong field region. Taking the scalar product of the relativistic equation of motion with momentum $\boldsymbol{p}$, we have

$$\frac{d}{dt}\left(\frac{p^2}{2}\right) = q_i \boldsymbol{p}\cdot\boldsymbol{E}. \tag{10}$$

We obtain the magnitude of an energy jump by integrating Eq. (10) along the unperturbed orbit in the strong field region. We can use the unperturbed orbit because the particle energy is supposed to be quite large.[22] Particle orbit in a constant magnetic field $\boldsymbol{B}_1$ may be described as

$$x(t) = v_{\parallel}t\cos\theta_1 + \rho\sin\theta_1\cos(-\omega_{ci}t+\eta) + a_x, \tag{11}$$

$$y(t) = \rho\sin(-\omega_{ci}t+\eta) + a_y, \tag{12}$$

$$z(t) = v_{\parallel}t\sin\theta_1 - \rho\cos\theta_1\cos(-\omega_{ci}t+\eta) + a_z, \tag{13}$$

where θ_1, η, a_x, a_y, and a_z are constant. In the presence of electric fields, effects of the $\boldsymbol{E}\times\boldsymbol{B}$ drift may be added to Eqs. (11)–(13). The magnitude of the drift velocity is, however, supposed to be much smaller than the speed of fast ions. The momentum is then given as

$$p_x(t) = p_{1\parallel}\cos\theta_1 + p_{1\perp}\sin\theta_1\sin(-\omega_{ci}t+\eta), \tag{14}$$

$$p_y(t) = -p_{1\perp}\cos(-\omega_{ci}t+\eta), \tag{15}$$

$$p_z(t) = p_{1\parallel}\sin\theta_1 - p_{1\perp}\cos\theta_1\sin(-\omega_{ci}t+\eta). \tag{16}$$

If we substitute Eqs. (11)–(16) in Eq. (10) and integrate over time from $t = t_{\mathrm{in}}$ to $t = t_{\mathrm{out}}$, we obtain the increase in p^2 as

$$\begin{aligned}\delta\left(\frac{p^2}{2}\right) = {} & q_i p_{1\parallel}E_{\parallel}(t_{\mathrm{out}}-t_{\mathrm{in}}) - \frac{2q_i p_{1\perp}}{\omega_{ci}} \\ & \times (E_x\sin\theta_1 - E_z\cos\theta_1)\sin\left(-\frac{\omega_{ci}(t_{\mathrm{out}}+t_{\mathrm{in}})}{2}+\eta\right) \\ & \times\sin\left(-\frac{\omega_{ci}(t_{\mathrm{out}}-t_{\mathrm{in}})}{2}\right) + \frac{2q_i p_{1\perp}}{\omega_{ci}}E_y \\ & \times\cos\left(-\frac{\omega_{ci}(t_{\mathrm{out}}+t_{\mathrm{in}})}{2}+\eta\right)\sin\left(-\frac{\omega_{ci}(t_{\mathrm{out}}-t_{\mathrm{in}})}{2}\right).\end{aligned} \tag{17}$$

Here, $E_{\parallel} = E_x\cos\theta_1 + E_z\sin\theta_1$; here, contribution of B_y is neglected, which is small compared with B_z and B_x. The first term on the right-hand side can be neglected, because $E_{\parallel}$ is

usually small in magnitude in magnetohydrodynamic waves and changes sign as one moves from the shock ramp to the strong field region. (In these calculations, contributions from the thin shock ramp are not included.) If both (2) and (8) are satisfied, then the quantity $(v_{sh}-\langle v_x\rangle)(t_{out}-t_{in})$ should be small compared with ρ, where $\langle v_x\rangle$ is the average velocity in the x direction; $\langle v_x\rangle \sim v_\parallel \cos\theta$. It then follows that

$$-\pi-(-\omega_{ci}t_{in}+\eta)\simeq(-\omega_{ci}t_{out}+\eta)-(-\pi). \tag{18}$$

That is,

$$\cos\left(-\frac{\omega_{ci}(t_{out}+t_{in})}{2}+\eta\right)\simeq -1. \tag{19}$$

Then, Eq. (17) is reduced to

$$\delta\left(\frac{p^2}{2}\right)=-\frac{2q_ip_{1\perp}}{\omega_{ci}}E_y\sin\left(-\frac{\omega_{ci}(t_{out}-t_{in})}{2}\right). \tag{20}$$

Equation (20) gives an amount of energy that a fast particle gains per one gyroperiod. The energy increase depends on the time period $t_{out}-t_{in}$. Obviously, when

$$\omega_{ci}(t_{out}-t_{in})\simeq\pi, \tag{21}$$

it takes its maximum value,

$$\delta(p^2/2)=2q_ip_{1\perp}E_y/\omega_{ci}. \tag{22}$$

A fast particle can undergo energy jumps given by Eq. (22) many times in one shock wave.

It is interesting to note that the right-hand side of Eq. (22) increases with increasing particle energy. From the relation $\gamma=[1+p^2/(m_i^2c^2)]^{1/2}$, we have

$$\delta\gamma=\frac{1}{m_i^2c^2\gamma}\delta\left(\frac{p^2}{2}\right). \tag{23}$$

We substitute Eq. (22) in Eq. (23). Then, since both $p_{1\perp}$ $(=m_i\gamma v_\perp)$ and $1/\omega_{ci}$ are proportional to γ, we find

$$\delta\gamma\sim\alpha v_\perp\gamma, \tag{24}$$

where α is a constant. Because $v_\perp$ is supposed to be of the order of c, this relation between the energy γ and energy increase $\delta\gamma$ nearly coincides with the one assumed in the Fermi acceleration model;[8] even though the two mechanisms are different. The statistical study of this mechanism, i.e., acceleration by many shock waves, will thus be quite interesting. We here, however, restrict ourselves to the processes occurring in one shock wave.

III. SIMULATION

A. Simulation method and parameters

We now study the acceleration numerically. Since the simulation method was described in detail in the previous papers,[22,25] we only briefly mention it.

We use a one-dimensional (one space coordinate and three velocity components), relativistic, electromagnetic, particle simulation code with full ion and electron dynamics.[31,32] The total system length is quite long; $L_x=8192\Delta_g$, where Δ_g is the grid spacing. This will enable us to observe long time behavior of waves and particles. All lengths and velocities in the simulations were normalized to Δ_g and $\omega_{pe}\Delta_g$, respectively, where ω_{pe} is the spatially averaged plasma frequency.

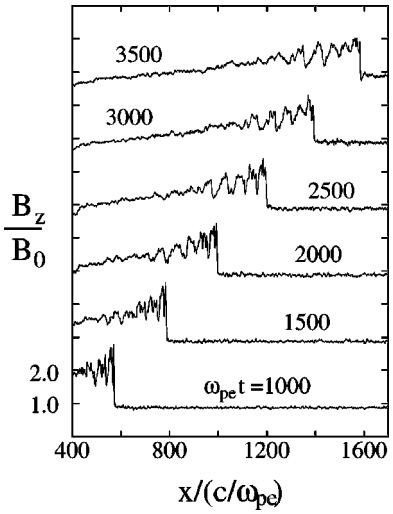

FIG. 5. Profiles of B_z of an oblique shock wave at various times.

As space plasmas, the code contains hydrogen (H), helium (He), and electrons. Ions consist of thermal bulk particles and nonthermal fast ones. The electrons and thermal ions initially have Maxwellian velocity distribution functions. All the fast ions initially have the same speed (same Lorentz factor γ_0) as isotropic momentum distributions. The abundance of the fast ions is quite small; in the present simulations it is one percent for each run.

The simulation parameters are the following: The ion-to-electron mass ratio is $m_H/m_e=50$; the speed of light is $c=4$; the electron skin depth is $c/\omega_{pe}=4$; the initial electron and ion thermal velocities are $v_{Te}=1.04$ and $v_{TH}=v_{THe}=0.04$, respectively. The frequency ratio ω_{ce}/ω_{pe} is 1.5 in the upstream region; thus, the Alfvén speed is $v_A=0.79$. The ratio between the two ion-cyclotron-frequencies is $\omega_{cH}/\omega_{cHe}=2$. The mass-density ratio is $n_{He}m_{He}/(n_Hm_H)=0.4$. The number of electrons is $N_e=576\,000$. The time step Δt is typically $\omega_{pe}\Delta t=0.05$, so that Δt is much smaller than the plasma and cyclotron periods even in the shock region. The external magnetic field is in the (x,z) plane, and waves propagate in the x direction. The angle θ $(\tan\theta=B_{z0}/B_{x0})$ was taken to be $\theta=61°$.

B. Simulation results

We show in Fig. 5 profiles of B_z in an oblique shock wave at various times. The shock speed is observed to be $v_{sh}=2.13v_A$; hence, the relation for the incessant acceleration, $c\cos\theta\sim v_{sh}$, is satisfied. Figure 6 displays the field profiles at $\omega_{pe}t=2000$. Note that B_z and E_y greatly increase in the shock region. The x component of $\boldsymbol{B}$, which is not shown here, is constant.

In this run, the initial Lorentz factor of fast ions was $\gamma_0=2$. We show in Fig. 7 time variations of x, γ, $p_\parallel$, $p_\perp$, and $v_{\parallel x}$ $(=v_\parallel B_{x0}/B)$ of a fast ion particle accelerated repeatedly. Here, x, p, and $v_{\parallel x}$ are normalized to c/ω_{pe}, m_ic, and c, respectively. In the top panel, the solid and dotted lines

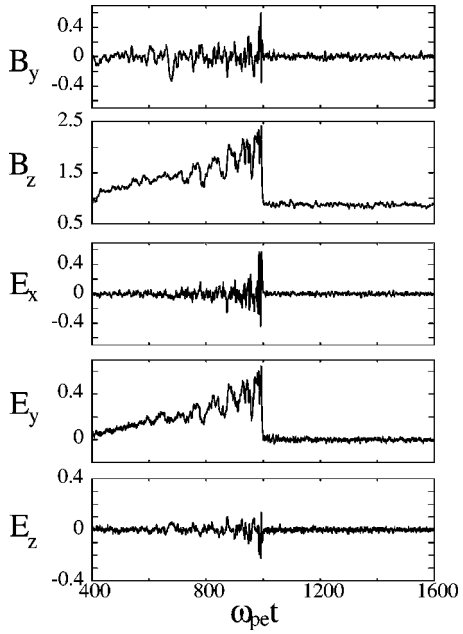

FIG. 6. Snapshots of field profiles. Electric and magnetic field profiles at $\omega_{pe}t=2000$ are plotted. They are normalized to B_0.

represent, respectively, the x position of the particle and leading edge of the shock wave at which B_z begins to sharply rise. The particle encounters the shock wave at $\omega_{pe}t=150$. It then quickly goes back to the upstream region owing to the gyromotion and soon enters the shock region again. This process is repeated many times with nearly the gyroperiod,

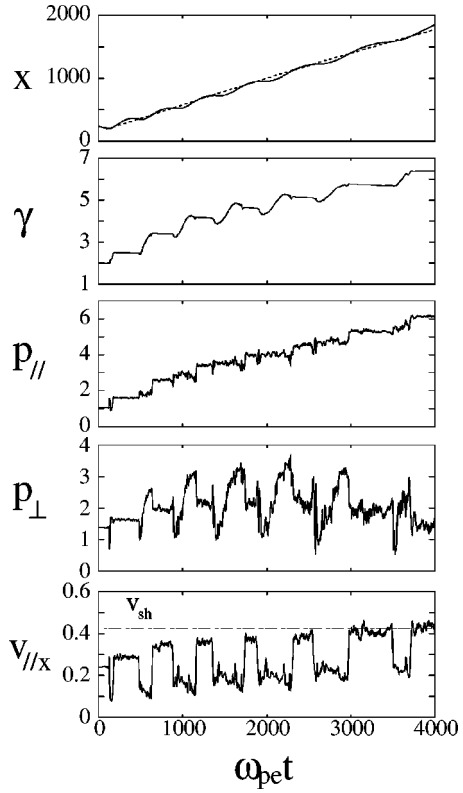

FIG. 7. Time variations of x, γ, $p_\parallel$, $p_\perp$, and $v_{\parallel x}$ of a fast ion being repeatedly accelerated.

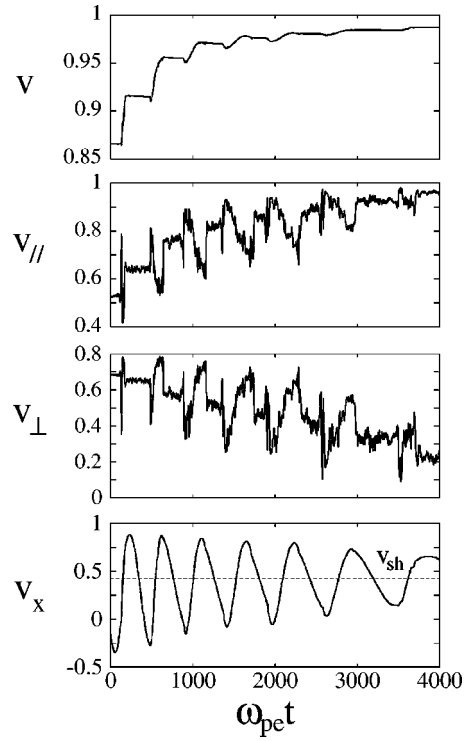

FIG. 8. Time variations of v, $v_\parallel$, $v_\perp$, and v_x.

which gradually becomes longer because the particle energy is increased. The second panel shows that the energy γ increases stepwise when the particle is in the shock region. During the run, the energy jumped seven times. When the simulation was finished, i.e., at $\omega_{pe}t=4000$, the particle was still moving with the shock wave and the process was continuing. The perpendicular momentum $p_\perp$ greatly increases when γ increases; right before and after this change, $p_\perp$ decreases and $p_\parallel$ increases. In other words, when the particle is in the strong field region, it gains energy from the electric field E_y. At the moment when it goes in or goes out of the shock region, $p_\parallel$ increases and $p_\perp$ decreases with the energy unchanged. The quantity $v_{\parallel x}$ takes small values in the shock region and large values in the upstream region, because B_z is large in the strong field region. From the bottom panel, therefore, we see the times when the particle is in the strong field region. Also, it shows a measure of average particle velocity in the x direction. In particular, when the particle is in the upstream region where the motions induced by $\boldsymbol{E}$ are not present, $v_{\parallel x}$ is exactly the time-averaged v_x.

Figure 8 displays time variations of v, $v_\parallel$, $v_\perp$, and v_x for the same particle. They are all normalized to c. The speed v increases stepwise with time, as the energy γ does. However, the magnitude of jump gradually decreases since v is limited by the speed of light c. The parallel speed also increases with time and becomes close to c. In contrast, $v_\perp$ slowly decreases with time, even though it gets larger when the particle is in the shock region. This is a reflection of the fact shown in Fig. 7 that $p_\parallel$ increases steadily with time, whereas $p_\perp$ only fluctuates around a roughly constant value. The bottom panel shows v_x. It is oscillating, and its average value is approaching the shock speed; $v_{\rm sh}$ is indicated by the

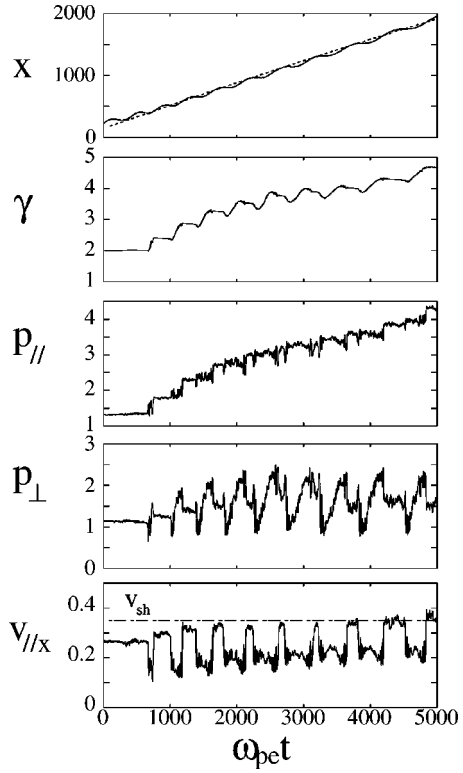

FIG. 9. Another example of accelerated particle. Here, time variations of x, γ, $p_{\parallel}$, $p_{\perp}$, and $v_{\parallel x}$ are shown. The propagation angle is $\theta=66°$, and the shock speed is $v_{\mathrm{sh}}=1.82v_{\mathrm{A}}$.

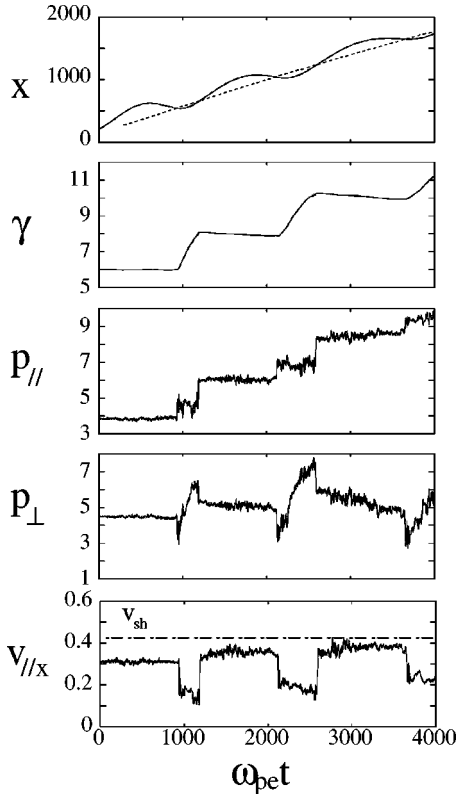

FIG. 10. Time variations of x, γ, $p_{\parallel}$, $p_{\perp}$, and $v_{\parallel x}$ of an accelerated fast ion. Its initial energy is $\gamma_0=6$.

dotted line. This suggests that the process would have continued for a longer period of time if the simulation was not terminated at $\omega_{pe}t=4000$.

We show in Fig. 9 another example of repeated acceleration. In this case, a fast particle is accelerated nine times. The propagation angle here is $\theta=66°$, and the shock speed is $v_{\mathrm{sh}}=1.82v_{\mathrm{A}}$. The other parameters are the same as the previous ones. The features of the change in x, γ, $p_{\parallel}$, $p_{\perp}$, and $v_{\parallel x}$ described in Figs. 7 are also observed in this case.

As indicated by Eq. (22), the magnitude of an energy jump can be large if the initial energy is high. Figures 10 and 11 demonstrate this. We examined cases with initial energy $\gamma_0=6$ (Fig. 10) and $\gamma_0=10$ (Fig. 11), with the other parameters the same as those in Fig. 7. Because γ is large, the gyroperiod and gyroradius are both much larger than the previous ones.

IV. SUMMARY AND DISCUSSION

By using a one-dimensional, relativistic, electromagnetic, particle simulation code, we have studied incessant acceleration of nonthermal, fast ions by a shock wave propagating obliquely to a magnetic field. We focused on the case where some fast ions cannot escape from the shock wave because of relativistic effects; in which indefinitely repeated acceleration is expected.

If there are fast ions with $v_{\parallel}\cos\theta<v_{\mathrm{sh}}$ in front of a shock wave, they will be caught up with by the shock wave. Then, some of them can gain energy from the transverse electric field formed in the wave; in this process, $p_{\perp}$ and γ increase simultaneously. In addition, just before and after the energy jump of a particle, i.e., at the moments when it goes in and out of the shock region, $p_{\parallel}$ (and hence $v_{\parallel}$) increases. This results from the fact that B_z is large in the shock region; the energy γ is therefore unchanged in this process. The average velocity in the x direction, $\sim v_{\parallel}\cos\theta$, then becomes higher, and the particle gets to move with the shock wave. If these processes (increase in γ and $p_{\parallel}$) are repeated a few times and if $c\cos\theta\gg v_{\mathrm{sh}}$, then the particle would escape, going away ahead of the shock wave, because $v_{\parallel}\cos\theta$ becomes larger than the shock speed v_{sh}. The acceleration then ceases.

However, if the condition $c\cos\theta\sim v_{\mathrm{sh}}$ is satisfied, the fast particle moving with a shock wave cannot go ahead of the wave. That is, they cannot escape from the shock wave because $v_{\parallel}\cos\theta$ cannot exceed the shock speed v_{sh}; the particle speed (and hence $v_{\parallel}$) is always lower than the speed of light c. As a result, the acceleration processes, increase in γ and $p_{\parallel}$, could be repeated indefinitely.

Indeed, our simulations have demonstrated that if the condition $c\cos\theta\sim v_{\mathrm{sh}}$ is satisfied, then some fast ions can move with the shock for extremely long periods of time. The acceleration processes took place many times in an oblique shock wave; when the simulation was terminated, the processes were still going on. It was also observed that the amount of an energy jump increases with the particle energy.

The acceleration was not finished during the simulation runs with a finite system size. It will thus be an important subject of future research to investigate the attainable maximum energy for specific situations. A possible mechanism limiting the acceleration is the decrease in the shock propa-

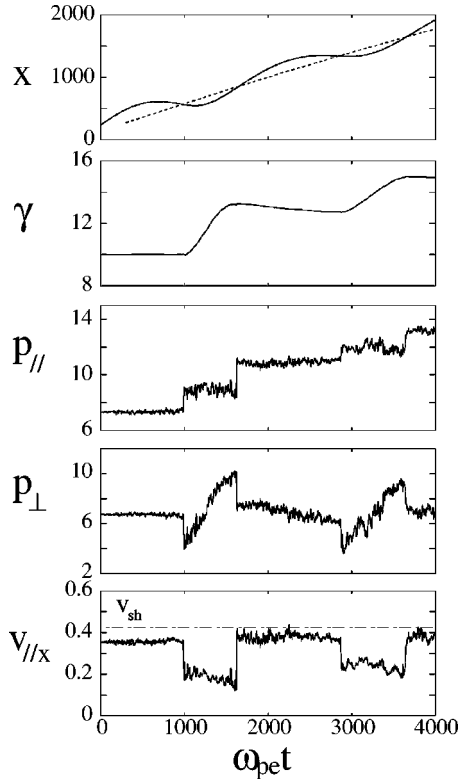

FIG. 11. Time variations of x, γ, $p_{\parallel}$, $p_{\perp}$, and $v_{\parallel x}$ of a fast ion with $\gamma_0 = 10$.

gation speed. Because $v_{\parallel}$ does not decrease in this mechanism, the particle would go ahead of the wave if the shock propagation speed is reduced. The decrease in the shock amplitude or in the Alfvén speed will lead to the slowing down of the shock speed. Also, if the gyroradius is extremely large, the acceleration processes may suffer some modification.

ACKNOWLEDGMENTS

This work was carried out by the joint research program of the Solar-Terrestrial Environment Laboratory, Nagoya University.

[1] E. L. Chupp, H. Debrunner, E. Flückiger *et al.*, Astrophys. J. **318**, 913 (1987).
[2] K. Koyama, R. Petre, E. V. Gotthelf *et al.*, Nature (London) **378**, 255 (1995).
[3] T. Tanimori, Y. Hayami, S. Kamei *et al.*, Astrophys. J. Lett. **497**, L25 (1998).
[4] T. Tanimori, K. Sakurazawa, S. A. Dazeley *et al.*, Astrophys. J. Lett. **492**, L33 (1998).
[5] R. A. Mewaldt, R. S. Selesnick, J. R. Cummings, E. C. Stone, and T. T. von Rosenvinge, Astrophys. J. Lett. **466**, L43 (1996).
[6] T. Tajima and J. M. Dawson, Phys. Rev. Lett. **43**, 267 (1979).
[7] C. Joshi, C. E. Clayton, W. B. Mori, J. M. Dawson, and T. Katsouleas, Comments Plasma Phys. Control. Fusion **16**, 65 (1994).
[8] E. Fermi, Phys. Rev. **75**, 1169 (1949).
[9] Y. A. Gallant and A. Achterberg, Mon. Not. R. Astron. Soc. **305**, L6 (1999).
[10] J. Bednartz and M. Ostrowski, Mon. Not. R. Astron. Soc. **310**, L11 (1999).
[11] J. G. Kirk and P. Duffy, J. Phys. G **25**, R163 (1999).
[12] D. Biskamp and H. Welter, Nucl. Fusion **12**, 663 (1972).
[13] D. W. Forslund, K. B. Quest, J. U. Brackbill, and K. Lee, J. Geophys. Res., [Oceans] **89**, 2142 (1984).
[14] Y. Ohsawa, Phys. Fluids **28**, 2130 (1985).
[15] Y. Ohsawa, J. Phys. Soc. Jpn. **55**, 1047 (1986).
[16] B. Lembege and J. M. Dawson, Phys. Fluids B **1**, 1001 (1989).
[17] R. L. Tokar, S. P. Gary, and K. B. Quest, Phys. Fluids **30**, 2569 (1987).
[18] M. Toida and Y. Ohsawa, J. Phys. Soc. Jpn. **64**, 2038 (1995).
[19] M. Toida and Y. Ohsawa, Sol. Phys. **171**, 161 (1997).
[20] N. Bessho and Y. Ohsawa, Phys. Plasmas **6**, 3076 (1999).
[21] N. Bessho and Y. Ohsawa, Phys. Plasmas **7**, 4004 (2000).
[22] K. Maruyama, N. Bessho, and Y. Ohsawa, Phys. Plasmas **5**, 3257 (1998).
[23] T. P. Armstrong, G. Chen, E. T. Sarris, and S. M. Krimigis, in *Study of Traveling Interplanetary Phenomena*, edited by M. A. Shea and D. F. Smart (Reidel, Dordrecht, 1977), p. 367.
[24] R. B. Decker, Space Sci. Rev. **48**, 195 (1988).
[25] T. Masaki, H. Hasegawa, and Y. Ohsawa, Phys. Plasmas **7**, 529 (2000).
[26] R. Z. Sagdeev and V. D. Shapiro, Zh. Eksp. Teor. Fiz. Pis'ma Red. **17**, 387 (1973) [JETP Lett. **17**, 279 (1973)].
[27] Y. Ohsawa, J. Phys. Soc. Jpn. **59**, 2782 (1990).
[28] M. A. Lee, V. D. Shapiro, and R. Z. Sagdeev, J. Geophys. Res. [Oceans] **101**, 4777 (1996).
[29] T. Kakutani, H. Ono, T. Taniuti, and C. C. Wei, J. Phys. Soc. Jpn. **24**, 1159 (1968).
[30] Y. Ohsawa, Phys. Fluids **29**, 1844 (1986).
[31] P. C. Liewer, A. T. Lin, J. M. Dawson, and M. Z. Caponi, Phys. Fluids **24**, 1364 (1981).
[32] Y. Ohsawa and J. M. Dawson, Phys. Fluids **27**, 1491 (1984).